© 1981 IEEE. Personal use of this material is permitted. However, permission to reprint/republish this material for advertising or promotional purposes or for creating new collective works for resale or redistribution to servers or lists, or to reuse any copyrighted component of this work in other works must be obtained from the IEEE.

IEEE Transactions on Nuclear Science, Vol. NS-28, No. 3, June 1981

PERFORMANCE OF INTENSE PULSED ION SOURCE*

T.C. Christensen and Z.G.T. Guiragossian

TRW, Defense & Space Systems Group
Advanced Technology Laboratory
One Space Park, Redondo Beach, CA 90278

Summary

The development of intense pulsed plasma ion sources for high current extraction of He^+, Ne^+ and Xe^+ beams is motivated by several applications. Cold (T_i < 0.2 eV) He^+ ions extracted at current density of 1-1.5 A/cm^2 across a 1 m radius surface for a total current of 25 kA in 0.5 μs pulses are required for a Light Ion Fusion Experiment (LIFE) ICF driver[1] based on the neutralized and ballistically focused propagation[2] approach. Moderate temperature (T_i ∿ 3 eV) Ne^+ and Xe^+ ions at 1-1.5 A/cm^2 for 1-10 A extracted currents in ms long pulses are required in several recent low β approaches based on multi-aperture quadrupole focused RF acceleration schemes such as the MEQALAC and the RFQ injector. In a test ion source, plasma is induced by ms time pulsing a 0.3 MHz, 0.1 MW RF oscillator with power AC-coupled to an antenna situated inside a 30 cm radius cylindrical vessel where the interior surfaces are lined with cusp-field permanent magnets except for the front extraction face. The plasma parameters T_e, T_i, n_p are characterized by measurements as a function of time during ms long pulses and in the immediate afterglow, the neutral gas density, the RF power and location at the extraction surface, and data are compared with derived scaling relations. The test source is pulsed at 10 Hz, mechanical design is simple, electrical efficiency is 20%, the source is rugged and has no delicate components which could limit performance time, and can be readily scaled in size. The induced plasma densities are strongly dependent on gas pressure and antenna coupled RF power; in the range of 10^{-3}-5x10^{-3} torr and 0.4 - 0.8 MW, experimental data and scaling relations show that 1 - 1.5 A/cm^2 current densities can be extracted for He^+, Ne^+, Ar^+ and Xe^+ beams from comparable source geometries. Ion temperatures cool down rapidly by ion-neutral collisions to T_i < 0.2 eV in 20 μs time in the afterglow, producing a quiescent plasma sheath at extraction, while ion densities remain relatively unchanged. The source can be used in the afterglow mode for μs beam pulse extraction or in the induction mode for long duration beams injected into low β multi-aperture RF linacs.

Performance of Pulsed Plasma Ion Source

The operation of the test source facility is shown in Fig. 1 and the experimental arrangement is sketched in Fig. 2. The pulsed source operates by the use of RF heating a low density initiated plasma in a vessel where the confinement of plasma electrons is aided by surface cusp-field permanent magnets. A single low power filament is used to initiate the plasma. Since high RF power levels can be coupled to a large plasma volume in a pulsed mode, inducing densities in excess of 10^{13} cm^{-3} for several ms duration at a rate matching the cycling of an accelerator system, low average power is consumed by the source and dissipated in the structures. Electron emission from the low power filament seeds a plasma by gas breakdown which is ∿ 10^4 times amplified by avalanching electrons accelerated to higher energies by means of the induced axial electric field of the RF antenna. The cusp magnetic field at the walls returns these primary electrons to cause additional ionization, enhancing the path length of electrons which are subsequently lost after about ten reflections from the walls. Other magnetic fields are not employed which would otherwise complicate the extraction optics. The only requirement of the RF power source is that oscillator frequency should be much smaller than the plasma ion frequency, $f_{RF} \ll f_{pi}$; $f_{pi} \simeq 330$ MHz for $n_p = 10^{13}$cm^{-3} in He, so that $f_{RF} \sim 1$ MHz is acceptable. The antenna consists of a few turns of copper tubing which may have a thin insulation surface. The antenna acts as the reactive element in a tuned tank circuit driven by a grid-pulsed class C oscillator. An impedance matching transformer AC-couples the RF power and matches the power source impedance to the plasma impedance. The antenna is situated some 30 cm away from the extraction surface. At 100 kW coupled power, the peak-to-peak

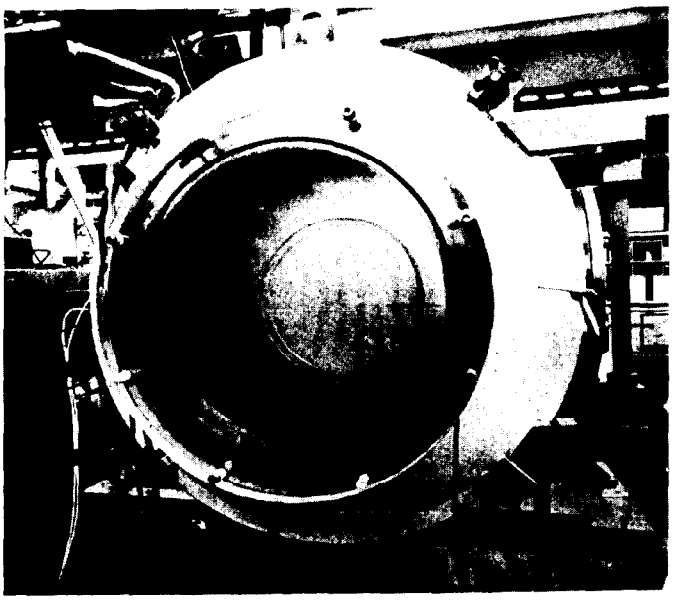

Figure 1. Performance of the Test Ion Source.

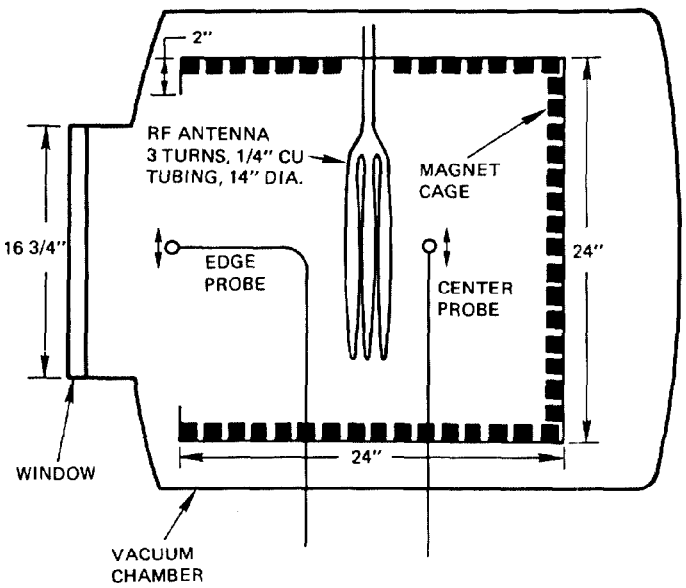

Figure 2. Experimental Setup of the Pulsed Intense Cold Plasma Ion Source.

0018-9499/81/0600-2666$00.75©1981 IEEE

values of voltage is 2 kV and current is 400 A at the antenna for 1 ms pulses at ∿ 10 Hz. Plasma build up as a function of time after RF power is triggered on is given by

$$n_p(t) = n_e(1 - e^{-C_s t/R}) \quad (1)$$

where R = V/A, V is the plasma vessel volume, A is the effective plasma vessel wall area including the multipole magnet effects, $C_s = c(T_e/M_i)^{1/2}$ and n_e is the steady state plasma density. n_e is a function of the RF power P, the electron energy required to create an ion-electron pair E_{i-e} and the frequency of ion loss at the walls $\nu_{iL} = 1/2\ C_s/R$:

$$n_e = \frac{2P}{ecE_{i-e}A}\left(\frac{M_i}{T_e}\right)^{1/2} . \quad (2)$$

E_{i-e} has contributions from the processes of ionization, excitation and kinetic losses. Assuming equal amounts of electron energy is lost to ionize and excite the neutral species and neglecting the excitation of ions, E_{i-e} is obtained:

$$E_{i-e} = 2\phi_i + \phi_p + 2\ (T_e + T_i) \quad (3)$$

where ϕ_i is the ionization potential (24.6 eV for He) and the plasma potential $\phi_p \equiv \gamma T_e$ is calculated by the equality of loss rates for electrons and ions dissipated at the walls, so that the constant factor is $\gamma = \ell n(2\sqrt{\pi m_e/8M_i})$. At steady state the ion loss rate is equal to the ion formation rate ν_i which is given by the rate of neutral gas ionization $\langle \sigma v_e \rangle_{o-i}$ and the gas density n_o: $\nu_i = n_o n_e \langle \sigma v_e \rangle_{o-i} = \nu_{iL}$. Consequently, the RF heated electrons attain a temperature value given by

$$T_e = M_i \left(n_o \langle \sigma v_e \rangle_{o-i}\ 2R/c\right)^2 \quad (4)$$

which is solved numerically, using the known noble gas ionization rate coefficients; T_e decreases with increasing n_o and from Eq. (2), n_e increases non-linearly with n_o and linearly with P. The emission limited extractable ion current density is,

$$J = 0.344\ n_p ec\left(2\ T_e/M_i\right)^{1/2} \quad (5)$$

so that hot electrons and high plasma densities are desired to have high current densities, while ion temperatures should be cold to help produce small emittance and high brightness ion beams. As shown by the results, these conflicting requirements are attained in a time window at the immediate afterglow regime of plasma induction. Thus, plasma build up to steady state levels occurs in 50 - 100 μs after RF power is triggered and $T_e \simeq$ 2-7 eV for Xe and He plasmas, respectively, at $n_o \simeq 10^{14}cm^{-3}$. (In the above, masses are in unit of eV/c^2, temperature and energy are in unit of eV).

Experimental Results

The plasma parameters n_p, T_e and T_i are measured as a function of P, n_o and t during induction and in afterglow. T_e is measured by determining the functional dependence of Langmuir probe current and voltage in terms of electron repelling voltages. n_e is measured with a 70 GHz microwave interferometer where radiation propagating across the plasma experiences a total phase shift proportional to the index of refraction which is a function of $n_e \cdot T_i$ is determined by measuring the Doppler broadening of a visible excitation line detected by a Fabry-Perot interferometer. T_i cooldown to room temperature is so rapid that this measurement could only be carried out with Argon plasma using photon counting techniques with proper isolation of mechanical and room temperature perturbations. Plasma electron density as a function of antenna coupled RF power is shown in Fig. 3 for three cases of Helium gas density. The scaling of n_e in terms of P and n_o is established. Higher plasma densities are obtained at higher gas densities, scaled almost linearly with RF power where due to burn-out, saturation occurs when $n_e \sim n_o$. In Fig. 4 data are presented in the afterglow regime where RF power at turn-off is 100 kW and Helium gas density is $1.5 \times 10^{14}cm^{-3}$. The plasma density decay and, T_e and T_i cooldown phenomena are characterized as a function of time in afterglow

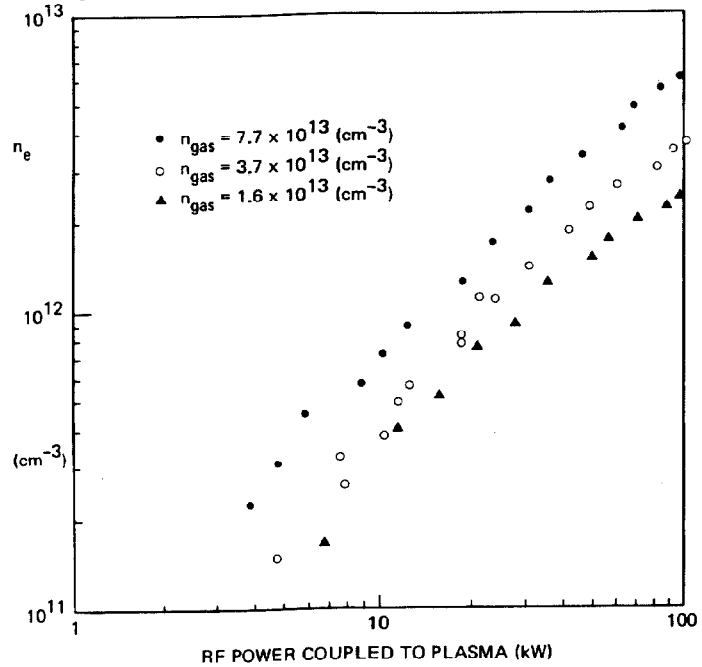

Figure 3. Measurement of RF Induced Pulsed Plasma Density in Helium as a Function of RF Power.

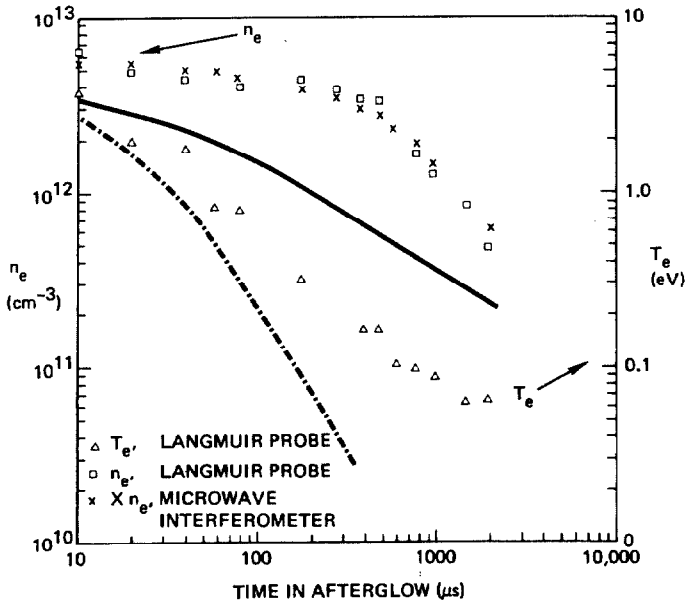

Figure 4. Measurement of Electron Temperature and Density as a Function of Time in the Afterglow of RF Induced Pulsed Plasma at 100 kW RF power and $1.5 \times 10^{14}cm^{-3}$ Helium Gas Density.

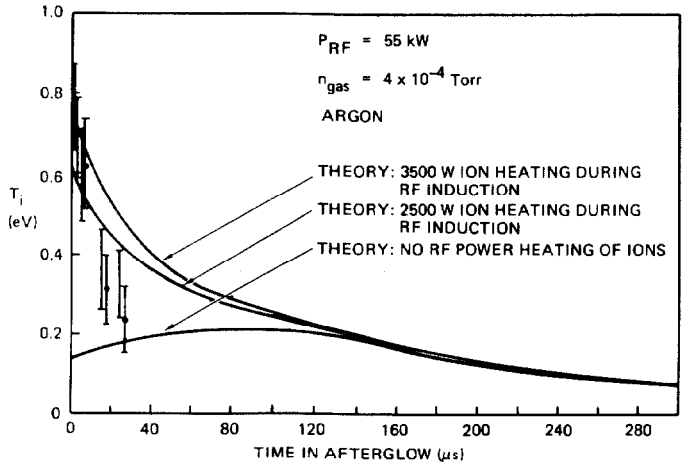

Figure 5. Measurement of Ion Temperature as a Function of Time in the Afterglow.

and compared to a theoretical model. The model is based on particle balance, electron energy balance and ion energy balance equations, as a function of time. Electron energy is lost to the walls, to ionization and excitation of neutrals and to heating of ions by elastic collisions; ion energy is lost to the walls and energy gain from electrons is overcompensated by energy transfer to neutrals, causing more rapid cooldown of T_i as compared to T_e. This is observed in Fig. 5 where the possibility of RF power coupling to the ions is also parameterized. In Fig. 4, T_e decreases far more rapidly in the afterglow than n_e, caused by the faster dissipation of hotter electrons to the walls and also because electron energy is lost to excitation of neutrals and ions. In Fig. 5, T_i decreases much more rapidly in the afterglow than T_e, due to the collisions of ions with cold neutrals, reaching $T_i \simeq 0.2$ eV in less than 30 μs while n_e remains relatively constant. The radial profile in n_e at the volume center plane and the front extraction plane is shown in Fig. 6; n_e is diminished by a factor of 2 from center to front. Inside a 15 cm wide radial edge band from the confinement surface magnets, n_e is uniform to within 10%. Thus, at P = 100 kW, extracted current density is 0.25 A/cm^2 for He^+ beams with $T_i \sim 0.2$ eV, corresponding to a total current of 100 A assuming an extraction radius of 15 cm with transparency to beams of 50%. Due to plasma potential oscillations T_i would be a few eV if ion extraction is carried out during the RF induction period of ms. Scaling from these results, 1-1.5 A/cm^2 He^+, Ne^+, Ar^+ and Xe^+ beams can be generated with P = 0.4 - 0.8 MW in comparable source geometries.

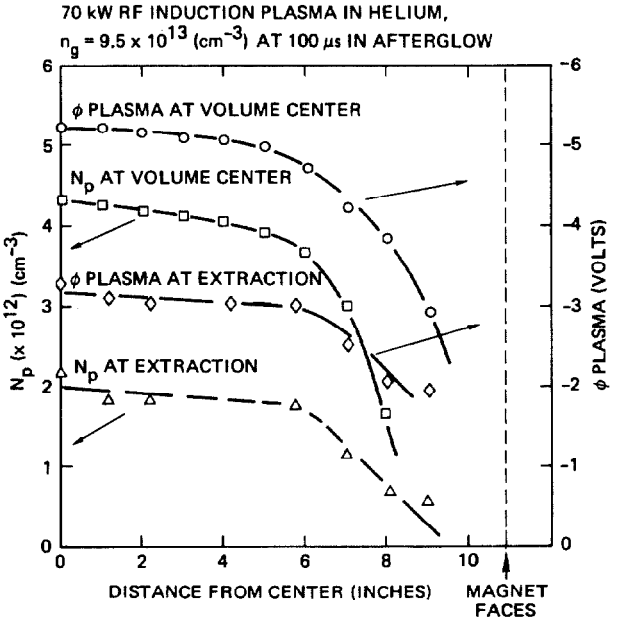

Figure 6. Measurement of Plasma Density Radial Profile at Extraction Surface and Volume Center.

*Work performed under the auspices of U.S. Army BMDATC Contract DASG60-79-C-0111.

1. Z.G.T. Guiragossian and J.L. Orthel, "Multi-Stage Intense Ion Beam Electrostatic Accelerator for ICF," in these proceedings.

2. Z.G.T. Guiragossian, J.L. Orthel, D.S. Lemons and L.E. Thode, "Method of Active Charge and Current Neutralization of Intense Ion Beams for ICF," in these proceedings.